CrossMark

ORIGINAL PAPER

Impedimetric immunoassay for aflatoxin B1 using a cysteine modified gold electrode with covalently immobilized carbon nanotubes

Maurilia P. Costa[1] · Isaac A. M. Frías[2] · Cesar A. S. Andrade[2,3] · Maria D. L. Oliveira[2,3]

Abstract The authors describe a label-free electrochemical biosensor based on CNTs for picogram range detection of the food carcinogen aflatoxin B1 (AFB1). A gold electrode was modified with a cysteine (Cys) self-assembled layer, and carboxyl-functionalized carbon nanotubes were covalently attached to Cys for the subsequent tethering of antibody against AFB1 (anti-AFB1). Topographical images of the biosensor surface were acquired by atomic force microscopy throughout the modification and assay procedure. Upon exposure to samples containing AFB1, its binding to anti-AFB1 will result in a change in electrical conductivity. The use of CNT warrants enhanced electrical properties, and the charge-transfer resistance (Rct) can be related to the concentration of AFB1. Biosensor selectivity was tested by using samples containing ochratoxin A. The electrode displays a limit of detection as low as 0.79 pg·g^{-1}, and response is linear in the 0.1 to 20 pg·g^{-1} concentration range. The assay was applied to the determination of AFB1 in contaminated corn flour at concentrations so low that they cannot be quantified by established ELISAs. In our

✉ Maria D. L. Oliveira
m_danielly@yahoo.com.br

[1] Programa de Pós-Graduação em Bioquímica e Fisiologia, Universidade Federal de Pernambuco, Recife, PE 50670-901, Brazil

[2] Programa de Pós-Graduação em Inovação Terapêutica, Universidade Federal de Pernambuco, Recife, PE 50670-901, Brazil

[3] Departamento de Bioquímica, Universidade Federal de Pernambuco, Recife, PE 50670-901, Brazil

perception, this method represents a viable point-of-care probe for detection of AFB1.

Introduction

Aflatoxin B1 (AFB1), produced by *Aspergillus* fungi of the genus *flavus* and *parasiticus* [2] is considered the most toxic aflatoxin and potential carcinogen classified in Group 1 according to International Agency for Research on Cancer [3]. Foodstuff and animal feed [4] including cereals, legumes, groundnut and corn have important role as complementary foods and are extremely vulnerable to AFB1 contamination [5]. International maximum limits for aflatoxins present in foodstuff are 50 pg·g^{-1} applied for food safety and health of the population [6]. In European countries, the highest permissible AFB1 concentration for food intended for direct human consumption is 10 ng g^{-1}. For instance, its maximum tolerated level in maize is 5 ng·g^{-1}, whereas in other foods as milk the limit is set to 5 pg·g^{-1} [7–9].

Thin layer chromatography, liquid chromatography, immunoaffinity chromatography, high-performance liquid chromatography and enzyme-linked immunosorbent assay (ELISA) are the most widely employed analytical techniques for the identification and quantification of aflatoxins [10]. Additionally, immunoassays are recognized as highly sensitive for AFB1 assessment in food and agricultural products. The lowest reported LOD for AFB1 using ELISA kits is 2 pg·g^{-1} [11]. However, these methods are time consuming, require special equipment, trained

personnel and additional pretreatment of the sample. As a result, biosensors arise as an essential alternative developed to be rapid, practical and economical methods towards AFB1 detection. Besides specific antigen-antibody immunoreaction, other receptors such as aptamers are emerging. Aptamers are single-stranded oligonucleotides specifically raised to target molecules [12]. Although their production is easier and less expensive in comparison to antibodies, antibody industrial production is already largely stablished and therefore easier to implement. Several nanomaterials are used as supporting transducers or tracers that amplify the detection signal of immunosensors and immunoassays, recent results are summarized in a thorough review [13]. Carbon nanotubes (CNT) are nanoparticles exhibiting exceptional surface/volume ratio that enables improved immobilization of biomolecules for the development of sensor devices. Additionally, carbon nanostructures can be multifunctionalized to be used as suitable scaffolds to tether molecular probes onto them. In the last five years, CNT-conjugates have been employed as biosensing platforms to detect and transduce the recognition response of cell-surface glycans [14, 15], enzymes and protein receptors [16], DNA and chylomicrons [17, 18]. However, CNT-based immunosensors are considered to be still in the early stage of development, requiring further investigation [19]. Recently, it has been demonstrated that multiwall CNT transducers enhance oxidation signals [20], thus propelling electrochemical CNT-based biosensors development.

The present work describes the construction of a label-free electrochemical immunosensor based in carboxyl-functionalized multiwall carbon nanotubes for detecting AFB1 in corn flour samples. A homogeneously distributed self-assembled cysteine (Cys) layer proved to be an efficient linker for CNT. AFB1 monoclonal antibodies (anti-AFB1) are directly tethered to the nanostructured film by covalent linkages. Sensitivity and selectivity of the biosensor were studied by cyclic voltammetry (CV), electrochemical impedance spectroscopy (EIS) and atomic force microscopy (AFM). Interference was studied by testing ochratoxin A (OTA) contaminated corn flour samples. OTA is a nephrotoxic and carcinogenic mycotoxin produced by species of Aspergillus in warmer climates of the South America and Africa. Compared to current immunological methods, the system is fast to construct, selective and stands out as a highly sensitive point-of-probe monitoring biosensor. It may help agricultural producers to enhance the yield of current crop stocking methods. Other methods such as immunochromatographic strips [42] are also easier to use and simpler to analyze, although their sensitivity and limit of detection (LOD) prevents their use as monitoring tools, since their positive result would represent the loss of the product.

Experimental

Materials

Potassium ferrocyanide and potassium ferricyanide $K_4[Fe(CN)_6]/K_3[Fe(CN)_6]$, 1-ethyl-3-(3-dimethylaminopropyl)carbodiimide (EDC), N-hydroxysuccinimide (NHS), multiwalled CNT, bovine serum albumin (BSA), Cys, monoclonal antibody anti-AFB1, AFB1 and OTA were purchased from Sigma-Aldrich (St. Louis, USA http://www.sigmaaldrich.com). Corn flour samples contaminated with AFB1 and OTA were purchased from Neogen Food Safety (Lansing, USA http://foodsafety.neogen.com). All chemicals and solvents were of analytical grade and used as received, without further purification.

Construction of the immunosensing platform

A gold electrode (BGE) was polished with 0.05 μm α-Al₂O₃ paste and carefully cleaned by rinsing and set in an ultrasonic bath in ultrapure water for 10 min. Cleaning procedure was repeated each time after exposure to samples during electrochemical characterization and testing. Modification process of Cys-CNT-Anti-AFB1-BSA-modified electrode is shown n Fig. 1. Initially, 3 μL of a 15 mM Cys solution was carefully dropped over the BGE and allowed a 20-min incubation time at 25 °C to create a self-assembled layer (Fig. SI.1). Subsequently, the electrode was set in an ultrasound bath for 1 min. Cys-CNT system was constructed by wise-dropping 3 μL of an aqueous solution containing carboxyl-CNT diluted in a 1:1 of a EDC (0.4 M), NHS (0.1 M), and carefully incubated for 50 min at 25 °C. Afterwards, 3 μL of a 25 mg mL⁻¹ Anti-AFB1 solution diluted in 1:1 EDC: NHS was added dropwise over the activated platform and let to incubate for 40 min at 25 °C (Fig. SI.2.). Finally, the remaining nonspecific sites were blocked with 1 μL of a 10% w/v BSA solution incubated for 5 min. After this point, the biosensor is ready to be exposed to AFB1 samples.

Detection of AFB1 in standard and corn flour samples

The biosensing ability of the Cys-CNT-Anti-AFB1-BSA-modified electrodes was evaluated by use of standard solutions adjusted at different concentrations of pure AFB1 [0.1, 1.0, 3.0, 6.0, 9.0, 11.0 and 20.0 pg·g⁻¹], 2 μL were added dropwise and let to incubate for 15 min at 25 °C. Corn flour samples spiked with AFB1 (0.1, 5.0, 9.0, 11.0 and 15.0 pg·g⁻¹ concentrations) were used to evaluate the sensitivity of the sensor. In addition, corn flour samples spiked with OTA [0.1, 5.0, 10.0 and 15.0 pg·g⁻¹] were used as negative control to evaluate the specificity of the immunosensor. Validated protocols detailing aflatoxin extraction from grain samples usually appoints methanol or water-methanol solutions as solvents [21]. Thus, to
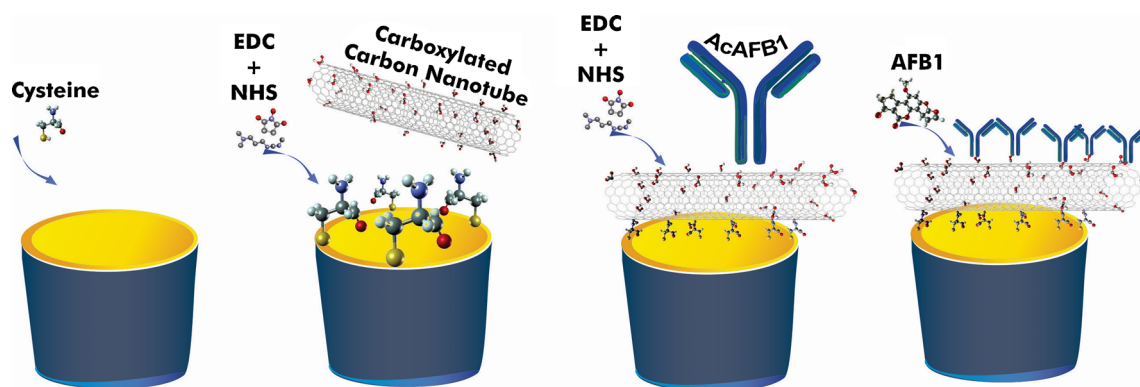
Fig. 1 Schematic construction of AFB1 immunosensor based on carbon nanostructures and cysteine for use in food safety

avoid interferences caused by the possible denaturation of Anti-AFB1 by interaction with alcohol, 1 g of each contaminated corn flour sample was first mixed in methanol, followed by clarification through centrifugation process. Subsequently, the supernatant was collected and evaporated according to Haskard et al. [22] with a slight modification on the heating temperature at 70 °C in a waterbath for 10 min. After this time, 1 mL of ultrapure water was added to the precipitate.

Electrochemical characterization

The electrochemical response of the biosensor was monitored throughout the construction process by using an Autolab PGSTAT 128 N potentiostat/galvanostat interfaced with NOVA 1.1 software (Metrohm Autolab Inc., Netherlands http://www.metrohm-autolab.com). All measurements were performed on a three-electrode-configured electrochemical cell and a 10 mM $K_4[Fe (CN)_6]/K_3[Fe(CN)_6]$ (1:1) solution redox probe solution was used for VC and EIS analyses in order to compare with previous published works [23–25]. Working solution was added with 10 mM PBS used as supporting electrolyte and pH was adjusted to 7.4 to provide maximum response according to a previous publication [26]. CV measurements were swept between −0.2 and +0.7 V at 50 mV·s^{-1} scan rate. Impedance measurements were performed in the range between 100 mHz to 100 kHz frequency under a + 10 mV sine wave potential. The gold electrode and its subsequent modifications were used as the working electrode, while a platinum and Ag/AgCl electrodes (in 3 M KCl) were used as counter and reference electrodes, respectively. All electrochemical measurements were triplicate repeated at room temperature inside a Faraday cage. The impedimetric responses were modelled using NOVA 1.1 software (Metrohm Autolab Inc., Netherlands) according to the equivalent circuit shown in inset of Fig. 3a. The modelled Cole-Cole diagrams present two distinct segments, a semicircle at higher frequencies, assigned to the electron transfer, and a posterior straight line occurring at lower frequencies attributed to the diffusion limited electron transfer process.

Topographical characterization

Surface characterization of the sensor was performed using an atomic force microscope (SPM-9500 J2; Shimadzu, Tokyo, Japan). Cantilevers with a silicon AFM probe (Tap190Al-G, 190 kHz resonant frequency, 48 N m^{-1} force constant) were used for the noncontact mode AFM in air at room temperature (approximately 25 °C). Lateral resolution was set to 512 × 512 pixels in a scan area of 10 × 10 μm. At least three areas in each sample were macroscopically separated for analysis. The AFM Gwyddion software was used to analyze the images [27].

Results and discussion

Topographical analyses

Figure 2 shows the changes in roughness of the electrode surface after the immunosensor assembly process. After incubation with cysteine, the molecules organize themselves in the form of a self-assembled monolayer (SAM) over the gold surface favored by the terminal thiol groups of Cys (Fig. 2a). In Fig. 2a, an effective Cys dense film modifying the surface topography with a height of 24 nm is observed. Compared to previous reported works [28, 29], a similar height of this new topography is confirmed, however, this method results in a more dense and homogeneous film. After the covalent anchorage of CNT on Cys layer, a distinctive change in height to 96 nm is observed (Fig. 2b). After Anti-AFB1 immobilization, the average height increased to 110 nm (Fig. 2c). However, a smoother morphology with an average height of 136 nm is observed after blocking nonspecific sites with BSA. Cys-CNT-Anti-AFB1-BSA surface becomes more homogeneous (Fig. 2d). The Cys-CNT-Anti-AFB1-BSA-AFB1 immunosensor after exposure to an AFB1-contaminated corn flour sample at 15.0 pg·g^{-1} concentration is shown in Fig. 2e. In addition, a drastic change in the morphology of the surface including a height increase to 440 nm is observed. This
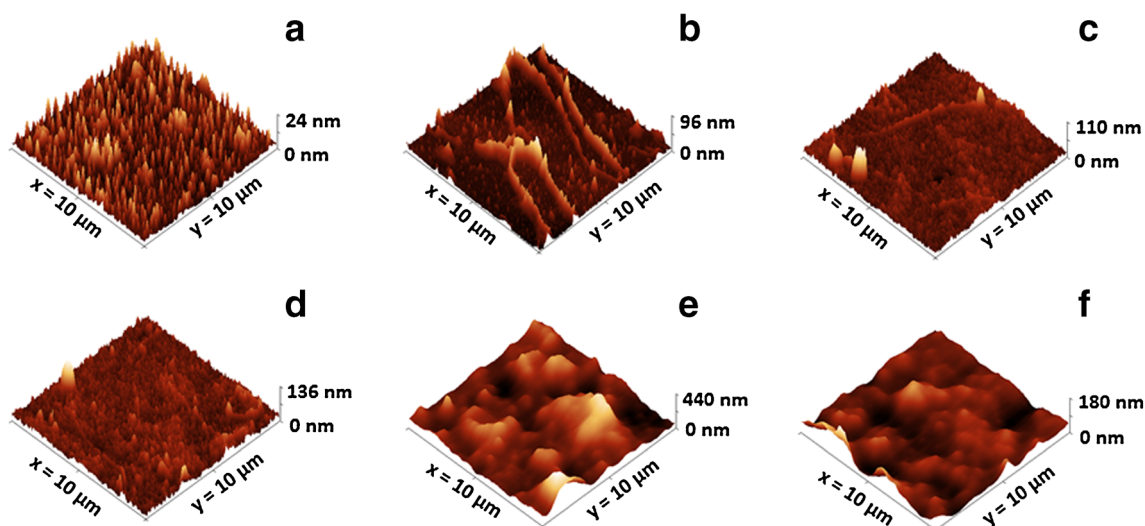
Fig. 2 3D AFM images of Cysteine SAM (**a**), Cys-CNT (**b**), Cys-CNT-Anti-AFB1 (**c**), Cys-CNT-Anti-AFB1-BSA (**d**), Cys-CNT-Anti-AFB1-BSA-AFB1 as positive sample (**e**) and Cys-CNT-Anti-AFB1-BSA-OTA as negative sample (**f**). Scan area of 10 μm × 10 μm

behavior confirms that, even after being adsorbed on the surface of carbon nanotubes, Anti-AFB1 retained its bioactivity. As an experiment control, the surface of the Cys-CNT-Anti-AFB1-BSA immunosensor after being exposed to an OTA-contaminated corn flour sample at 15.0 pg·g^{-1} concentration (Fig. 2f) is shown. As expected, no significant height change was observed. Thus, the specificity of the constructed immunosensor towards other mycotoxins is verified.

Electrochemical characterization

After each assembly step, one can observe an increase in the diameter of the Nyquist semicircle that is directly related to the Rct. The response is a result of the antigen-antibody complex, thus contributing to our findings about the maintenance of Anti-AFB1 bioactivity, even after being adsorbed on the surface of carbon nanotubes [30]. The BGE impedimetric response is mainly related to diffusion processes with Rct values equivalent to 249 Ω. Cys-CNT-Anti-AFB1 system presents an increase in impedimetric response (Rct = 4.03 kΩ) due to a shielding effect of the layer avoiding the electrochemical probe transfer. Next, when the immunosensor is exposed to an AFB1 positive sample, the captured molecules provide an additional blocking layer that decreases the redox probe flux nearby the transducer.

Changes in voltammetric behavior during the construction stages of the biosensor are shown in Fig. 3b. The initial BGE signal presents a reversible voltammogram compatible to the response of the redox probe. Thus, diffusion processes control the reactions that lead the electron transfer. After modifying the electrode to obtain the immunosensor, we notice a decrease in the amperometric response in accordance with the hampered motility of the redox probe towards the transducer found in the impedimetric results. After exposing the

immunosensor to an AFB1 sample, a drastic decrease of the oxidation/reduction signals is observed, including a separation of the anodic and cathodic peaks. Despite the observed quasi-reversible behavior, the gathered results suggest that the deceleration of the redox couple transfer rate towards the transducer is proportional to the amount of surface coating.
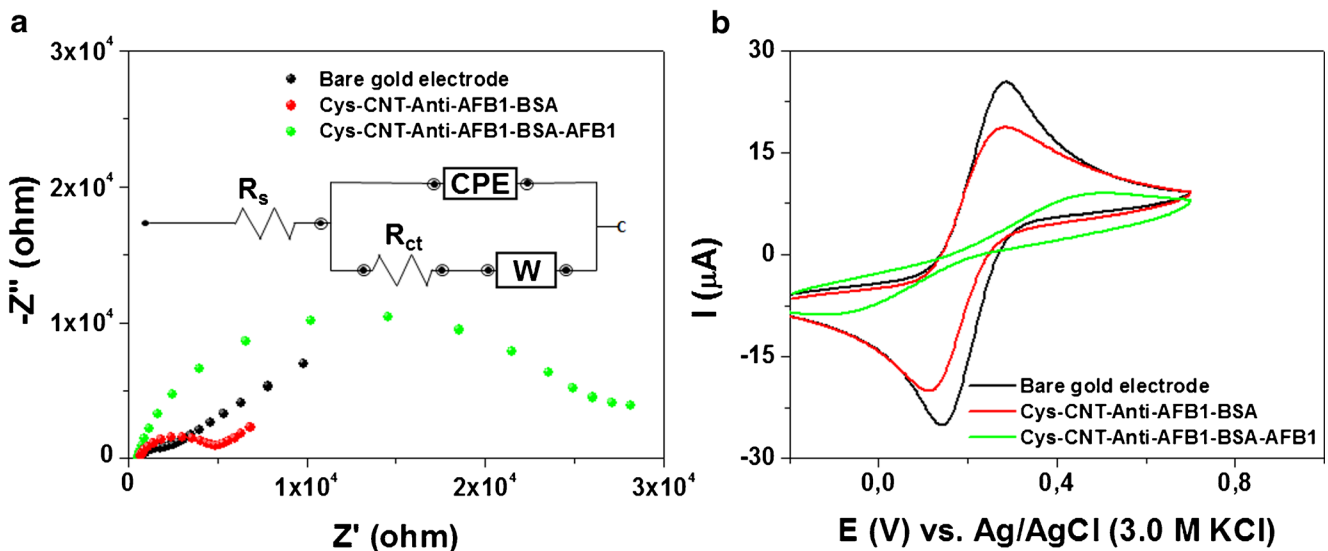
Sensitivity of the immunosensor

To assess reproducibility and standard experimental deviation (S.D.), the following data is presented as the result of three replicates performed for each sample. Sensitivity was evaluated by creating a calibration curve from the EIS responses resulting from the exposure of the immunosensor to pure standard AFB1 samples.

In Fig. 4a we present the impedimetric responses of the immunosensor after its exposure to AFB1 standard solutions at the following concentrations: 0.1, 1.0, 3.0, 6.0, 9.0, 11.0, 15.0 and 20.0 pg·g^{-1}. The scattered points represent the experimental results while the solid black lines show the fitting curves resultant from the equivalent circuit (Fig. 4a). From the first sample detection (0.1 pg·g^{-1}), one can see a gradual increase in Rct resistance from 6.97 to 84.33 kΩ (20.0 pg·g^{-1}).

The results of modeled the data with basis in the equivalent circuit are shown in Table SI.1. Since the most altered parameter is the Rct, it is convenient to evaluate the antigen-antibody interaction in terms of the relative variation of the Rct as defined by:

$$\%\Delta Rct = \left| \frac{Rct_{CNT-antiAFB1-AFB1} - Rct_{CNT-antiAFB1}}{Rct_{CNT-antiAFB1}} \right| x\, 100 \quad,$$

According to this equation, the Rct$_{CNT\text{-}antiAFB1}$ corresponds to the initial immunosensor response and Rct$_{CNT\text{-}antiAFB1\text{-}AFB1}$

Fig. 3 Nyquist plots (**a**) and cyclic voltammograms (**b**) for each step in the assembling of the immunosensor. Inset: Equivalent circuit used to fit the impedance results

is the charge transfer resistance of the biosensor response after its interaction with AFB1. Sensitivity and reproducibility were assessed from the relationship existing between ΔRct % and the concentration of AFB1 and its plot is shown in Fig. 4b. The linear relationship was modelled by ΔRct % = 98.19 + 92.38 [AFB1 pg·g^{-1}] with a coefficient of determination of 0.99. From the impedimetric analysis, LOD was estimated based on the S.D. of the responses and the calculated slope as follows: LOD = 3.3 σ·s^{-1}. In this expression, *s* is the slope of the calibration curve and σ, is the S.D. of the intercept of the regression line. The LOD value obtained (0.79 pg·g^{-1}) was a lower value than that found in current AFB1 tests run by ELISA (2 pg·g^{-1}) and lower than recent AFB1-detecting molecular biosensors ranging from 3.5 pg·g^{-1} to 5 ng·g^{-1} [25, 31–35].

Selectivity of the immunosensor, analysis of corn flour samples

Selectivity was assessed by testing the immunosensor towards corn flour samples contaminated with AFB1 for positive samples and OTA for negative samples. Figure 5a presents the impedimetric responses of the immunosensor after exposure to corn flour samples contaminated with AFB1 at different concentrations [0.1, 5.0, 9.0, 11.0, 15.0 pg·g^{-1}]. The incubation of the immunosensor with AFB1 samples resulted in an increase of the Rct, this behavior is associated to the redox probe being obstructed in its way towards the transductor interface.

The experimental bioactivity was analyzed through ΔRct% responses related to the concentration of the mycotoxins.
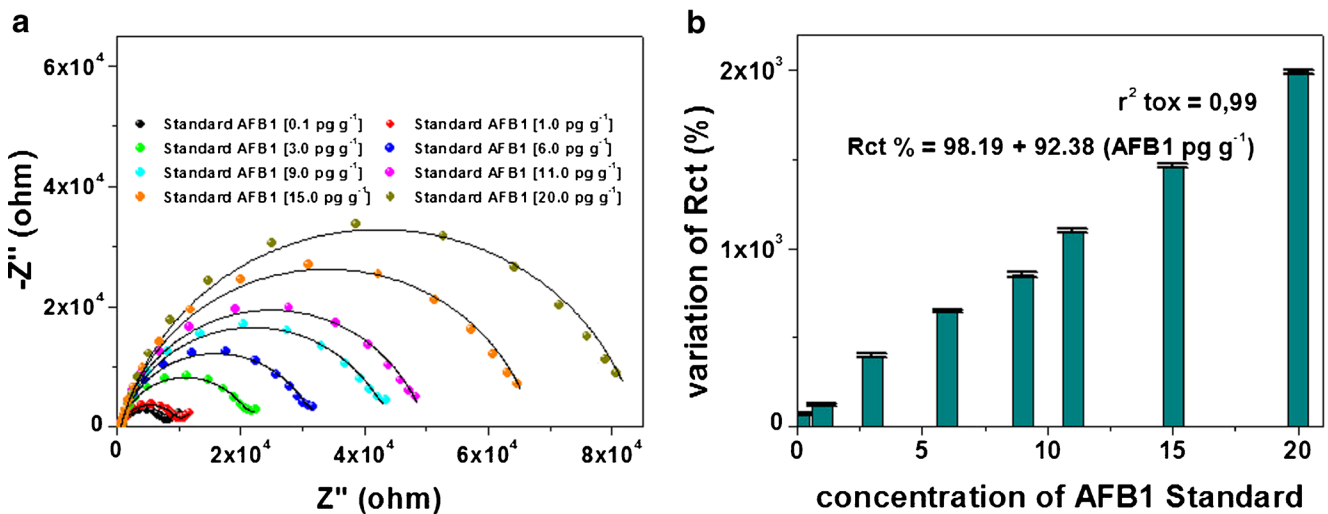
Fig. 4 Nyquist plots (**a**) and histogram of ΔRct (%) of the immunosensor (**b**) after exposure to different concentrations of AFB1 standard 0.1, 1.0, 3.0, 6.0, 9.0, 11.0, 15.0 and 20.0 pg·g^{-1}.

Three replicates for each experimental condition were used. Experimental values are reported as the mean values ± their half-deviation (less than 1%)

Fig. 5 Nyquist plots (**a**) and histogram showing the ΔRct (%) of the immunosensor after exposure to corn flour infected with AFB1 as positive samples [0.1, 5.0, 9.0, 11.0 and 15.0 pg·g⁻¹] (**b**) and with OTA as negative samples [0.1, 5.0, 10.0 and 15.0 pg·g⁻¹] (**c**). Three replicates for each experimental condition were used. Experimental values are reported as the mean values ± their half deviation (less than 1%)
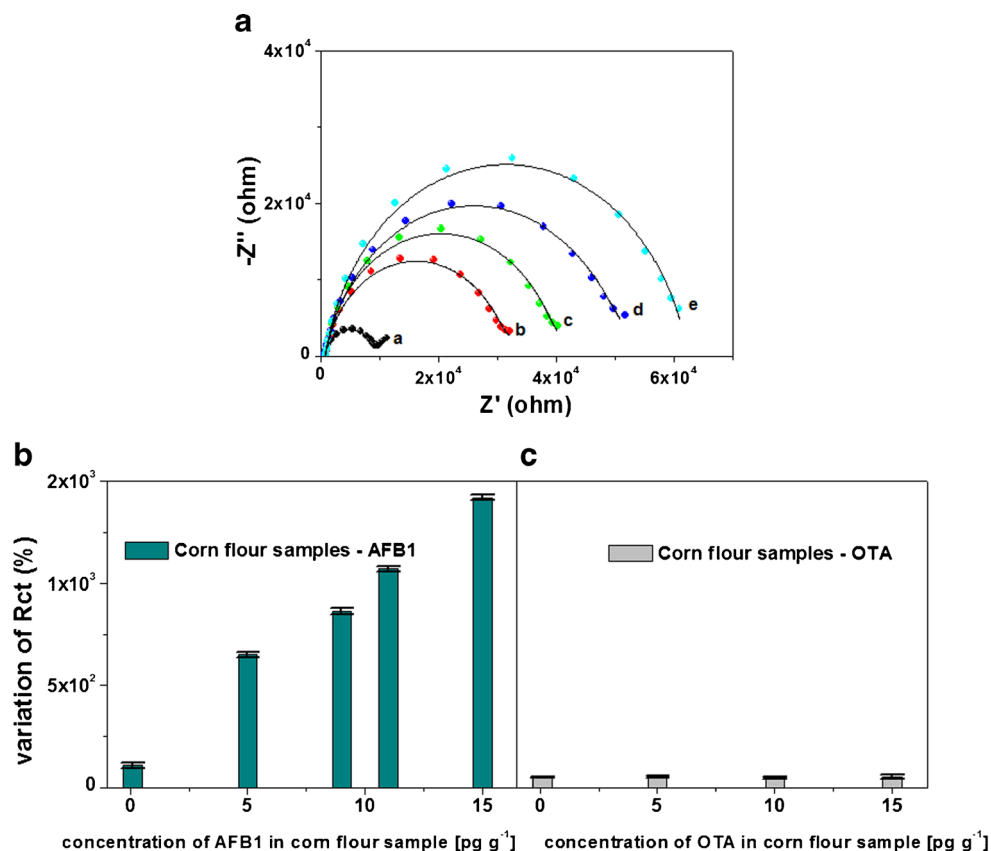
Table 1 Comparison of some analytical features of Label-Free CNT immunosensor for AFB1 to those of other immunosensors

Detection technique	Sensor type	Assay platform	Linear range	LOD	Construction/ measure (t)	Ref
Electrochemical	immunosensor	Graphene/conducting polymer/ gold Np/ionic liquid composite film	3.2–32 fg mL⁻¹	312 ag mL⁻¹	27 h/15 min	[40]
Electrochemical	immunosensor	SWCNT /chitosan	0.01–100 ng mL⁻¹	3.5 pg mL⁻¹	2 h/3.5 h	[31]
Electrochemical	immunoassay	Printed carbon electrode	0.125–16 ng mL⁻¹	125 pg mL⁻¹	3 h/15 min	[41]
Electrochemical	immunosensor	MWCNT /Polymer/Pd-Au nanoparticles	0.05–25 ng mL⁻¹	30 pg mL⁻¹	3 h/15 min	[23]
Surface plasmon resonance	immunosensor	Polymeric brushes/Au nanoparticles (NPs)	0.1 ng/mL μg mL⁻¹	18 pg mL⁻¹	13 h/55 min	[33]
Mechanical immunosensor	immunosensor	Gold surface	0.1–50 ng mL⁻¹	30 pg mL⁻¹	2 days/1 h	[34]
Optical/ fluorescence	immunosensor	Planar waveguide	73–400 pg mL⁻¹	45 pg mL⁻¹	5 h/20 min	[35]
Fluorescence	immunoassay	Quantum dots	0.1–0.6 μmol mL⁻¹	0.2 pmol mL⁻¹	8 h/3 min	[12]
Immunochromatographic strip	immunoassay	Nitrocelulose/ Antibodies	-	0.1 ng mL⁻¹	5 min	[42]
Portable electrochemical	immunosensor	Gold surface	5–20 ng mL⁻¹	5 ng mL⁻¹	4 h/1 h	[25]
Electrochemical impedance	Aptasensor	Thiolated aptamers	0.1–100 nmol mL⁻¹	0.12 ng mL⁻¹	-	[43]
Differential pulse voltammetry	Aptasensor	Printed/ magnetic Nps-Biotin Aptamer	1–50 ng mL⁻¹	0.11 ng mL⁻¹	-	[44]
Differential pulse voltammetry	Aptasensor	Thiolated aptmers/ labeled Fc	0.005–10 ng mL⁻¹	0.001 ng mL⁻¹	-	[45]
Electrochemical impedance	Immunosensor	Covalent/ Cys-MWCNT-AcAFB1	0.1–20 pg mL⁻¹	0.79 pg mL⁻¹	2 h/15 min	This work

Figure 5b shows the bioactivity of positive samples of corn flour contaminated with AFB1. In addition, the impedimetric result for negative samples of corn flour contaminated with OTA at different concentrations [0.1, 5.0, 10.0 and 15.0 pg·g^{-1}] is shown in Fig. 5c. Blue columns represent the ΔRct% found for AFB1 samples. As it can be observed, there is a large linear variation of the Rct from 107.9% to 1421.1% for the immunosensors exposed to AFB1 samples. On the other hand, the immunosensors exposed to OTA samples presented almost unchangeable ΔRct%, even at increasing concentrations, with 49.43% as mean value. This behavior categorically supports the selectiveness of our immunosensors besides supporting our findings about the maintenance of Anti-AFB1 bioactivity even after being covalently-immobilized onto the surface of the carbon nanotubes.

It is important to highlight that not all reported electrochemical platforms developed to detect AFB1 consider covalent immobilization of the antibody to the carbon material itself. For instance, in Table 1 we compare some analytical features of our system to those of other immunosensors. Of note, although physicochemical interactions are preferred, CNT-based transducers are relatively easy and fast to construct. Carbon-based transducers are the preferred option for electrochemical immunosensors. In addition, the reported time for a complete detection in these methods is also fast. The development of this immunosensor asserts the direct covalent immobilization of Anti-AFB1 to the CNT by initially constructing a dense Cys SAM that is able to immobilize a considerable amount of CNT nanostructures, increasing thus the amount of sites available for Anti-AFB1 binding. The presented methodology dispenses the use of unspecific ionic interactions to immobilize CNT as it is currently done with ionic matrixes, thus resting in CNT electrical properties [36, 37]. For the most probable, the simplicity and precision of our mounting methodology is essential to attain a 0.79 pg·g^{-1} LOD. In addition, our methodology was found to be among the mean preparation time of current electrochemical immunosensors with 2 h for construction and 15 min detection. Furthermore, our immunosensor was also comparable with other LOD reports on commercial AFB1 ELISA kits [38] (MyBioSource: 250 pg·g^{-1}; Quicking Biotech: 100 pg·g^{-1}; MaxSignal: 50 pg·g^{-1}; Diagnostic Automation: 5 pg·g^{-1}). It's worth highlighting that our system revealed a good sensitivity and performance when compared with sensors based on aptamers. In addition, some authors revealed that aptamer systems possesses difficult to detect AFB1 in real samples at low concentrations. Finally, the interest in using carbon nanomaterials in electrochemical platforms continues to grow at a fast pace [39], and improving their performance is essential to attain the sensitivity once predicted by theoretical works.

Conclusions

In this paper, we have presented a simple and sensitive impedimetric immunosensor for AFB1 detection based in a cysteine self-assembled layer, which was used for the covalent anchoring of carboxyl-functionalized CNTs. Compared to other nanostructured immunosensors, the preparation of our platform is simple an efficient. We improved the nanostructuration of the immunosensor by employing covalent interaction of the platform with the substrate, as a manner of increasing the resistance to peeling off. In this context, the incubation time and temperature control are critical parameters to attain the initial dense Cys film on which the subsequent tethering depend. Electrochemical characterization, CV and EIS, conjointly with AFM topographical analyses confirmed that the bioactivity of the antibodies is maintained after their covalent immobilization while maintaining high specificity towards AFB1. The system is sufficiently sensitive to dismiss the use of signal amplifiers. Despite improvements in terms of fast construction, surface coverage optimization and high specificity, our immunosensor is still difficult to regenerate working as a single time analysis, and therefore, the system has to be constructed from scratch each time before use. When compared to current traditional methods and alternative immunological biosensors, our biosensor showed fast fabrication (2 h) and operation (15 min) besides acceptable reproducibility (RSD < 5%). When testing AFB1 standards, the biosensor performed with a low LOD of 0.79 pg·g^{-1} and a linear detection range between 0.1 to 20 pg·g^{-1}. Such level of sensitivity in a portable label-free detector would facilitate in-field use, or for instance, alternative continuous quality monitoring of crop storages.

References

1. Abdel-Aziz SM, Asker MMS, Keera AA, Mahmoud MG (2016) Microbial food spoilage: control strategies for shelf life extension. In: Garg N, Abdel-Aziz MS, Aeron A (eds) Microbes in food and health. Springer International Publishing, Cham, pp 239–264. doi:10.1007/978-3-319-25277-3_13
2. Adebo OA, Njobeh PB, Gbashi S, Nwinyi OC, Mavumengwana V (2015) Review on microbial degradation of aflatoxins. Crit Rev Food Sci Nutr:00–00. doi:10.1080/10408398.2015.1106440

3. Lee J, Her J-Y, Lee K-G (2015) Reduction of aflatoxins (B1, B2, G1, and G2) in soybean-based model systems. Food Chem 189:45–51. doi:10.1016/j.foodchem.2015.02.013

4. Shephard GS (2016) Current status of mycotoxin analysis: a critical review. J AOAC Int 99(4):842–848. doi:10.5740/jaoacint.16-0111

5. Temba MC, Njobeh PB, Kayitesi E (2017) Storage stability of maize-groundnut composite flours and an assessment of aflatoxin B1 and ochratoxin A contamination in flours and porridges. Food Control 71:178–186. doi:10.1016/j.foodcont.2016.06.033

6. De Saeger S, Audenaert K, Croubels S (2016) Report from the 5th International symposium on mycotoxins and toxigenic Moulds: challenges and perspectives (MYTOX) held in Ghent, Belgium, May 2016. Toxins 8(5):146. doi:10.3390/toxins8050146

7. Juan C, Raiola A, Mañes J, Ritieni A (2014) Presence of mycotoxin in commercial infant formulas and baby foods from Italian market. Food Control 39:227–236. doi:10.1016/j.foodcont.2013.10.036

8. Khayoon WS, Saad B, Lee TP, Salleh B (2012) High performance liquid chromatographic determination of aflatoxins in chilli, peanut and rice using silica based monolithic column. Food Chem 133(2):489–496. doi:10.1016/j.foodchem.2012.01.010

9. Fu Z, Huang X, Min S (2008) Rapid determination of aflatoxins in corn and peanuts. J Chromatogr A 1209(1–2):271–274. doi:10.1016/j.chroma.2008.09.054

10. Selvaraj JN, Zhou L, Wang Y, Y-j Z, F-g X, X-f D, Liu Y (2015) Mycotoxin detection — recent trends at global level. J Integr Agric 14(11):2265–2281. doi:10.1016/S2095-3119(15)61120-0

11. Schwartzbord J, Severe L, Brown D (2016) Detection of trace aflatoxin M1 in human urine using a commercial ELISA followed by HPLC. Biomarkers:1–4. doi:10.1080/1354750X.2016.1203998

12. Lu Z, Chen X, Wang Y, Zheng X, Li CM (2015) Aptamer based fluorescence recovery assay for aflatoxin B1 using a quencher system composed of quantum dots and graphene oxide. Microchim Acta 182(3):571–578. doi:10.1007/s00604-014-1360-0

13. Wang X, Niessner R, Tang D, Knopp D (2016) Nanoparticle-based immunosensors and immunoassays for aflatoxins. Anal Chim Acta 912:10–23. doi:10.1016/j.aca.2016.01.048

14. Reichardt NC, Martin-Lomas M, Penades S (2013) Glyconanotechnology. Chem Soc Rev 42(10):4358–4376. doi:10.1039/C2CS35427F

15. Andrade CAS, Nascimento JM, Oliveira IS, de Oliveira CVJ, de Melo CP, Franco OL, Oliveira MDL (2015) Nanostructured sensor based on carbon nanotubes and clavanin A for bacterial detection. Colloids Surf B: Biointerfaces 135:833–839. doi:10.1016/j.colsurfb.2015.03.037

16. Luo X, Davis JJ (2013) Electrical biosensors and the label free detection of protein disease biomarkers. Chem Soc Rev 42(13):5944–5962. doi:10.1039/C3CS60077G

17. Saxena U, Das Asim B (2016) Nanomaterials towards fabrication of cholesterol biosensors: key roles and design approaches. Biosens Bioelectron 75:196–205. doi:10.1016/j.bios.2015.08.042

18. Yang N, Chen X, Ren T, Zhang P, Yang D (2015) Carbon nanotube based biosensors. Sensors Actuators B: Chemical 207, Part A:690–715. doi:10.1016/j.snb.2014.10.040

19. Tîlmaciu C-M, Morris MC (2015) Carbon nanotube biosensors. Front Chem 3:59. doi:10.3389/fchem.2015.00059

20. Shobha BN, Muniraj NJR (2015) Design, modeling and performance analysis of carbon nanotube with DNA strands as biosensor for prostate cancer. Microsyst Technol 21(4):791–800. doi:10.1007/s00542-014-2281-x

21. Asghar MA, Iqbal J, Ahmed A, Khan MA, Shamsuddin ZA, Jamil K (2016) Development and validation of a high-performance liquid chromatography method with post-column derivatization for the detection of aflatoxins in cereals and grains. Toxicol Ind Health 32(6):1122–1134. doi:10.1177/0748233714547732

22. Haskard CA, El-Nezami HS, Kankaanpää PE, Salminen S, Ahokas JT (2001) Surface binding of aflatoxin B(1) by lactic acid bacteria.

Appl Environ Microbiol 67(7):3086–3091. doi:10.1128/AEM.67.7.3086-3091.2001

23. Zhang S, Shen Y, Shen G, Wang S, Shen G, Yu R (2016) Electrochemical immunosensor based on Pd–Au nanoparticles supported on functionalized PDDA-MWCNT nanocomposites for aflatoxin B1 detection. Anal Biochem 494:10–15. doi:10.1016/j.ab.2015.10.008

24. Luna DMN, Avelino KYPS, Cordeiro MT, Andrade CAS, Oliveira MDL (2015) Electrochemical immunosensor for dengue virus serotypes based on 4-mercaptobenzoic acid modified gold nanoparticles on self-assembled cysteine monolayers. Sensors Actuators B Chem 220:565–572. doi:10.1016/j.snb.2015.05.067

25. Li Z, Ye Z, Fu Y, Xiong Y, Li Y (2016) A portable electrochemical immunosensor for rapid detection of trace aflatoxin B1 in rice. Anal Methods 8(3):548–553. doi:10.1039/C5AY02643A

26. Yu L, Zhang Y, Hu C, Wu H, Yang Y, Huang C, Jia N (2015) Highly sensitive electrochemical impedance spectroscopy immunosensor for the detection of AFB1 in olive oil. Food Chem 176:22–26. doi:10.1016/j.foodchem.2014.12.030

27. Nečas D, Klapetek P (2012) Gwyddion: an open-source software for SPM data analysis. Open Physics 10(1):181–188

28. Simão EP, Barbieri GJLS, Andrade CAS, Oliveira MDL (2016) Biosensor based on cysteine monolayer and monoclonal antibody for specific detection of aflatoxin B1 in Rice. J Braz Chem Soc 27:1040–1047

29. Huayhuas-Chipana BC, Gomero JCM, Sotomayor MDPT (2014) Nanostructured screen-printed electrodes modified with self-assembled monolayers for determination of metronidazole in different matrices. J Braz Chem Soc 25:1737–1745

30. Takeda S, Sbagyo A, Sakoda Y, Ishii A, Sawamura M, Sueoka K, Kida H, Mukasa K, Matsumoto K (2005) Application of carbon nanotubes for detecting anti-hemagglutinins based on antigen–antibody interaction. Biosens Bioelectron 21(1):201–205. doi:10.1016/j.bios.2004.08.030

31. Zhang X, Li C-R, Wang W-C, Xue J, Huang Y-L, Yang X-X, Tan B, Zhou X-P, Shao C, Ding S-J, Qiu J-F (2016) A novel electrochemical immunosensor for highly sensitive detection of aflatoxin B1 in corn using single-walled carbon nanotubes/chitosan. Food Chem 192:197–202. doi:10.1016/j.foodchem.2015.06.044

32. Lou X, Zhu A, Wang H, Wu J, Zhou L, Long F (2016) Direct and ultrasensitive optofluidic-based immunosensing assay of aflatoxin M1 in dairy products using organic solvent extraction. Anal Chim Acta 940:120–127. doi:10.1016/j.aca.2016.08.020

33. Karczmarczyk A, Dubiak-Szepietowska M, Vorobii M, Rodriguez-Emmenegger C, Dostálek J, Feller K-H (2016) Sensitive and rapid detection of aflatoxin M1 in milk utilizing enhanced SPR and p(HEMA) brushes. Biosens Bioelectron 81:159–165. doi:10.1016/j.bios.2016.02.061

34. Zhou X, Wu S, Liu H, Wu X, Zhang Q (2016) Nanomechanical label-free detection of aflatoxin B1 using a microcantilever. Sensors Actuators B Chem 226:24–29. doi:10.1016/j.snb.2015.11.092

35. Guo H, Zhou X, Zhang Y, Song B, Zhang J, Shi H (2016) Highly sensitive and simultaneous detection of melamine and aflatoxin M1 in milk products by multiplexed planar waveguide fluorescence immunosensor (MPWFI). Food Chem 197, Part A:359–366. doi:10.1016/j.foodchem.2015.08.109

36. Kachoosangi RT, Musameh MM, Abu-Yousef I, Yousef JM, Kanan SM, Xiao L, Davies SG, Russell A, Compton RG (2009) Carbon nanotube−ionic liquid composite sensors and biosensors. Anal Chem 81(1):435–442. doi:10.1021/ac801853r

37. Wang X, Hao J (2016) Recent advances in ionic liquid-based electrochemical biosensors. Sci Bull 61(16):1281–1295. doi:10.1007/s11434-016-1151-6

38. Li Q, Lv S, Lu M, Lin Z, Tang D (2016) Potentiometric competitive immunoassay for determination of aflatoxin B1 in food by using

antibody-labeled gold nanoparticles. Microchim Acta 183(10): 2815–2822. doi:10.1007/s00604-016-1929-x

39. Reverté L, Prieto-Simón B, Campàs M (2016) New advances in electrochemical biosensors for the detection of toxins: nanomaterials, magnetic beads and microfluidics systems. A review. Anal Chim Acta 908:8–21. doi:10.1016/j.aca.2015.11.050

40. Linting Z, Ruiyi L, Zaijun L, Qianfang X, Yinjun F, Junkang L (2012) An immunosensor for ultrasensitive detection of aflatoxin B1 with an enhanced electrochemical performance based on graphene/conducting polymer/gold nanoparticles/the ionic liquid composite film on modified gold electrode with electrodeposition. Sensors Actuators B Chem 174:359–365. doi:10.1016/j.snb.2012.06.051

41. Yugender Goud K, Catanante G, Hayat A, M S, Vengatajalabathy Gobi K, Marty JL (2016) Disposable and portable electrochemical aptasensor for label free detection of aflatoxin B1 in alcoholic beverages. Sensors Actuators B Chem 235:466–473. doi: 10.1016/j.snb.2016.05.112

42. Masinde LA, Sheng W, Xu X, Zhang Y, Yuan M, Kennedy IR, Wang S (2013) Colloidal gold based immunochromatographic strip for the simple and sensitive determination of aflatoxin B1 and B2 in corn and rice. Microchim Acta 180(9):921–928. doi:10.1007/s00604-013-1008-5

43. Castillo G, Lamberti I, Mosiello L, Hianik T (2012) Impedimetric DNA Aptasensor for sensitive detection of Ochratoxin A in food. Electroanalysis 24(3):512–520. doi:10.1002/elan.201100485

44. Barthelmebs L, Hayat A, Limiadi AW, Marty J-L, Noguer T (2011) Electrochemical DNA aptamer-based biosensor for OTA detection, using superparamagnetic nanoparticles. Sensors Actuators B Chem 156(2):932–937. doi:10.1016/j.snb.2011.03.008

45. Tong P, Zhang L, Xu J-J, Chen H-Y (2011) Simply amplified electrochemical aptasensor of Ochratoxin A based on exonuclease-catalyzed target recycling. Biosens Bioelectron 29(1):97–101. doi:10.1016/j.bios.2011.07.075